Arrhythmogenicity quantification of two genetic defects affecting I_{Kr} channel in AF patients

R. Belletti[1], L. Martinez Mateu[2], L. Romero Perez[1], E. Cherry[3], F. H. Fenton[4], J. Saiz[1]

[1] Centro de Investigación e Innovación en Bioingeniería, Universitat Politecnica de Valencia, Valencia, España, rbelletti@ci2b.upv.es, jsaiz@ci2b.upv.es

[2] Departamento de Teoría de la Señal y las Comunicaciones y Sistemas Telemáticos y Computación, Universidad Rey Juan Carlos, Madrid, Spain, laura.martinez.mateu@urjc.es

[3] School of Computational Science and Engineering, Georgia Institute of Technology, Atlanta, GA, USA, elizabeth.cherry@gatech.edu

[4] School of Physics, Georgia Institute of Technology, Atlanta, GA, USA, flavio.fenton@physics.gatech.edu

Abstract

Atrial fibrillation (AF) is the most common cardiac arrhythmia characterized by disorganized electrical activations of the upper chambers of the heart, leading to uncoordinated contraction and compromising the pumping action of the organ. AF risk factors include cardiovascular pathologies, endocrine disorders, advanced age, obesity, smoking and heritability. Genetic mutations affecting gene encoding for ion channel protein structures are in fact considered as cause of fibrillatory events in individuals who do not present any other co-morbidities.

In this work, two genetic mutations found in literature and affecting the alpha-subunit of the rapid delayed rectifier potassium channel are modelled, by reparametrizing the I_{Kr} current formulation and by fitting it to mutant experimental data. The modified potassium current was then incorporated into the Courtemanche-Ramirez-Nattel (CRN) model and single cell simulations have been performed to study the mutations' effects on action potential and current traces, as well as, restitution properties, in right and left atrium. Both mutations produced a shortening of the action potential duration at 90% of repolarization (APD_{90}), a higher current peak and lower APD values in the restitution curves. T895M yielded also to a reduction in the maximum slope of restitution curve.

Tissue patch simulations revealed that T895M and T436M provide a substrate to initiate and maintain re-entries during the 5 seconds of simulation. Rotor's meandering in T895M appears more stable with a less extended area and more regular pattern than in T436M. Investigation on 3D atria and torso models will be necessary to provide further insights in understanding the mechanisms behind these genetic mutations.

1. Introduction

Defects in genes encoding for ion channel protein structures have been studied extensively in the past few decades because of their potential role in arrhythmogenic events genesis in otherwise healthy individuals. Onset of atrial fibrillation in patient not affected by cardiovascular disorders or metabolic conditions has been in fact implicated to the presence of genetic mutations, which cause abnormal current conduction through the pore, thus impairing the delicate balance of inward and outward currents through the cell membrane. Genetic predispositions and heritability of AF have been thus added to the long list of common risk factors and in particular this conditions has been named 'Lone AF', accounting for 30% of current AF cases [1][2]. Even though it is not a life threatening disease, AF worldwide affects 1.5 - 2% of general population, leading to a poor quality of life and becoming a growing issue for the healthcare system [3]. In order to better understand the functioning of this pathology, in this study we focus on the modelling and simulation of the effects of two missense gain-of-function mutations, T895M and T436M, found in literature in a previous work by [4]. The two mutations under study were detected in two male patients affected by Lone AF, developed then into paroxysmal and chronic AF over years. The defects affected the KCNH2 gene, which encodes for the α-subunit of the rapid delayed rectifier potassium channels, Kv11.1, underlying the I_{Kr} current. Channels in presence of the mutations result in conducting larger amount of current with respect to the wild-type (WT) case and in a slower deactivation. The simulation study have been performed in order to assess the effects of the two mutations and their potential risk to become a substrate for initiation and maintenance of AF. Single cell and tissue patch simulations have been executed using the human atrial model by Courtemanche-Ramirez-Nattel (CRN) [5]. Results showed how apparently similar mutations affect the system in a different manner, pointing out the importance of a patient-specific approach, especially in the designing of a drug therapy, at treatment stage.

2. Material and Methods

The human atrial single cell model proposed by Courtemanche and colleagues in [5] has been used to reproduce both healthy and mutated behaviour of myocytes.

	RA	LA
g_{CaL}	1	0.9
g_{Kr}	1	2
g_{KACh}	1	1

Table 1. *Factors applied to currents' conductance to account for atrial heterogeneities*

Acetylcholine current (with [ACh] = 0.005 μM) has been introduced since its important role in atrial

ISBN: 978-84-09-25491-0, pags. 141- 144

electrophysiology, in particular in the myocytes' repolarization phase [6]. Atrial heterogeneities for right atrium (RA) and left atrium (LA) have been accounted by varying some currents' conductance as shown in ***Table 1***.

2.1. Potassium Current Parameterization

The rapid delayed rectifier potassium current formulation has been reparametrized to integrate mutant experimental data in the dynamics of the channel. Parameters to be applied in I_{Kr} equations were evaluated and chosen through a sensitivity analysis. This process allowed to reach a final parameters' configuration shown in (1) to (3), which resulted to be the one with the highest influence on the curves to be fitted.

$$I_{Kr} = \frac{P_1 \cdot g_{Kr} \cdot C_m \cdot x_R \cdot (V - E_K)}{1 + e^{\frac{V+15}{22.4}}} \quad (1)$$

$$\alpha_{x(r)} = 0.0003 \cdot \frac{(V+14.1)}{1 - e^{\frac{V+14.1}{-5}}} \quad (2)$$

$$\beta_{x(r)} = P_2 \cdot 7.3898 \cdot 10^{-5} \cdot \frac{(V - 3.3328 + P_3)}{e^{\frac{V-3.3328+P_3}{5.1237 \cdot P_4}} - 1} \quad (3)$$

Parameter tuning has been done accounting for relative changes within the WT and the experimental data of the mutations, which were digitalized along with their experimental ranges as reported in the original study.

2.2. Optimization Algorithm

Parameter estimation has been achieved with the use of a genetic algorithm, implemented in Python, with an initial population size of 100 individuals and a number of generations equal to 100. The most suitable method for selection, crossover and mutation has been chosen in order to find the best solution in this specific problem. Regarding the selection, the 'Roulette Select' method has been preferred because of its high searching power in the local parameter space, while as for regards the crossover, 'Mate' method has been employed. The mutation method used a Gaussian mutation operator with a mutation rate of 0.9. The cost function to be minimized has been defined as a weighted root-mean-square error, between simulated and experimental data. Elitism of individuals in every generation is introduced, allowing to keep unchanged the 10% of the most fitted individuals from generation to generation. The choice of such optimization algorithm is motivated by its high ability to spread in the entire parameter space, with a low probability of get stuck in a local minima.

2.3. Single Cell Simulation

CRN model incorporating the ACh current and mutations' dynamics in the I_{Kr} channel is then used to run single cell simulations applying a 20 pA/pF amplitude current stimulus for 2 ms at different basic cycle lengths (BCLs), both in RA and LA. After 60 pulses of stabilization, action potential (AP) and current traces properties at BCL 1000 ms have been studied and compared with WT case. Restitution curves (APDr) have been presented as APD_{90} respect to diastolic interval (DI), in order to study the dependency to pacing frequency, in presence of genetic mutations.

2.4. Tissue Simulation

Two-dimensional model of a tissue layer of dimension 5 x 5 cm^2 and 300 µm spatial resolution incorporated the modified version of CRN model reproducing the mutations' behaviour. The monodomain formalism has been solved using the Elvira software [7]. A 2 s stimulus current of 100 pA/pF amplitude has been applied on the tissue patch mesh, with a longitudinal conductivity of 0.0022 S/cm·pF and an anisotropy ratio equal to 0.35. Ten planar pulses at BCL 1000 ms were paced in order to stabilize the tissue model, then S1-S2 cross-field protocol has been used to study vulnerability of the tissue to re-entrant activity. Stimulus S2 has been applied at the left bottom corner of the tissue in a rectangular-like shape area in 5-s simulations, a sufficient time to get stable re entries in a simple tissue geometry. For those cases in which re-entries maintained up to the simulation time, spectral and phase analysis of the signals have been performed in order to compute dominant frequencies (DF) and to track rotors tips' trajectory. DF were computed as the highest peak in the power spectrum of the signal and tracking of rotors have been achieved computing singularity points from phase maps built on the simulated signal with the use of the Hilbert transform.

3. Results

3.1. Fitting of Experimental Data

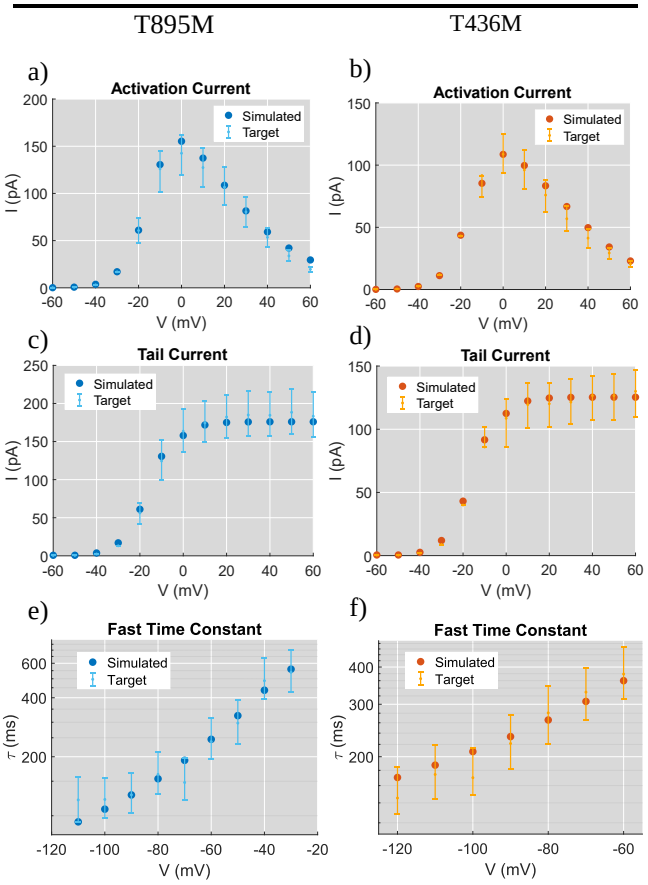

Figure 2. *Fitting procedure results. Comparison between experiments and simulations for* ***a)*** *and* ***b)*** *activation currents,* ***c)*** *and* ***d)*** *tail currents,* ***e)*** *and* ***f)*** *fast time constants, in T895M (blue) and T436M (orange) cases.*

The genetic algorithm successfully retrieve a set of parameter values realizing the adjustments to experimental data. Parameters that fit well the mutation datasets are shown in ***Table 2***.

T895M		T436M	
P_1	2.028	P_1	1.402
P_2	2.105	P_2	0.734
P_3	45.055	P_3	15.19
P_4	2.982	P_4	3.34

Table 2. *Parameters' values for T895M and T436M mutations*

Activation and tail currents, as well as time constants of the mutations, expressed with their experimental ranges, could be accurately adjusted to simulation data, as in ***Figure 2.***

3.2. Single Cell Simulation

Single cell simulations have been performed introducing the parameters shown in ***Table 2.*** in the formulation of the potassium current of the CRN model, along with factors accounting for atrial heterogeneities in ***Table 1.*** and ACh current formulation. Action potential and I_{Kr} current traces resulting from mutated models are shown and restitution properties are studied. Overall, the systems affected by the mutations presented a higher and earlier potassium current peak, which led to an action potential shortening. APDr were shifted to lower APD_{90} values in both cases, maintaining a rate-dependant behaviour.

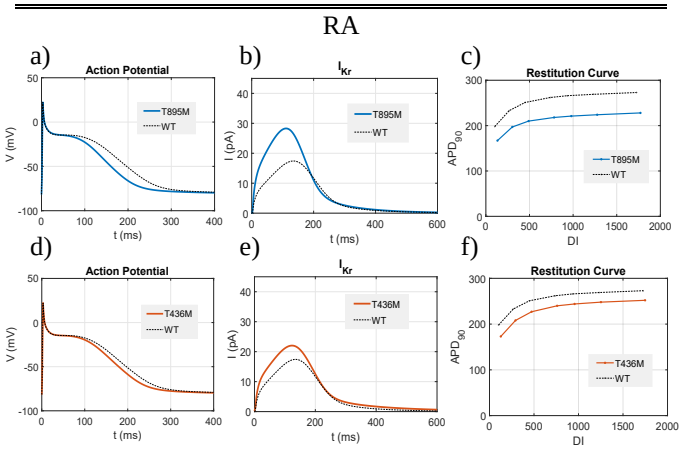

Figure 3. *Action potentials, I_{Kr} current and APDr in RA in presence of T895M (upper panel – solid blue lines) and T436M (lower panel – solid orange lines) compared to WT (dashed line).*

In right atrium, as shown in the upper panel of ***Figure 3.***, the mutation T895M yielded a reduction in the APD_{90} of 17% with respect to the control value, as a direct consequence to a 62% higher peak of the I_{Kr} current; moreover, potassium current time to peak is reduced by 24 ms. APDr in presence of T895M mutation appears flattened, with a 36% reduction in the maximum slope. In ***Figure 3.*** lower panel, results of the effects of T436M mutation in right atrium are depicted. APD_{90} shortens of about 8% the WT value, due to a current peak 26% higher and 12 ms earlier. Restitution curves maximum slope values did not show any difference respect to control case, but APD values were lowered. Results of the effects of the two mutations in left atrium single cell simulations are shown in ***Figure 4.***, where T895M and T436M are compared to control case. In case of T895M, APD is reduced by 23% the control value with a 60% higher current peak and a time to peak 25 ms earlier. APDr shifted to lower APD values and flattened its trend, reducing the maximum slope value of 31% with respect to WT case. The mutation T436M in LA yielded to an APD_{90} shortening of 12%, due to an increase in the potassium current peak of about 26%. As in RA case, APDr did not flattened and no changes in the maximum slope are reported.

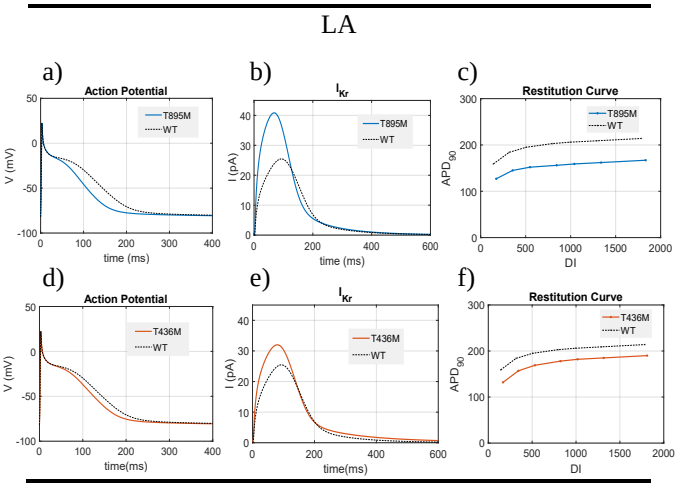

Figure 4. *Action potentials, I_{Kr} current and APDr in LA in presence of T895M (upper panel – solid blue lines) and T436M (lower panel – solid orange lines) compared to WT (dashed line).*

3.3. Tissue Patch Simulation

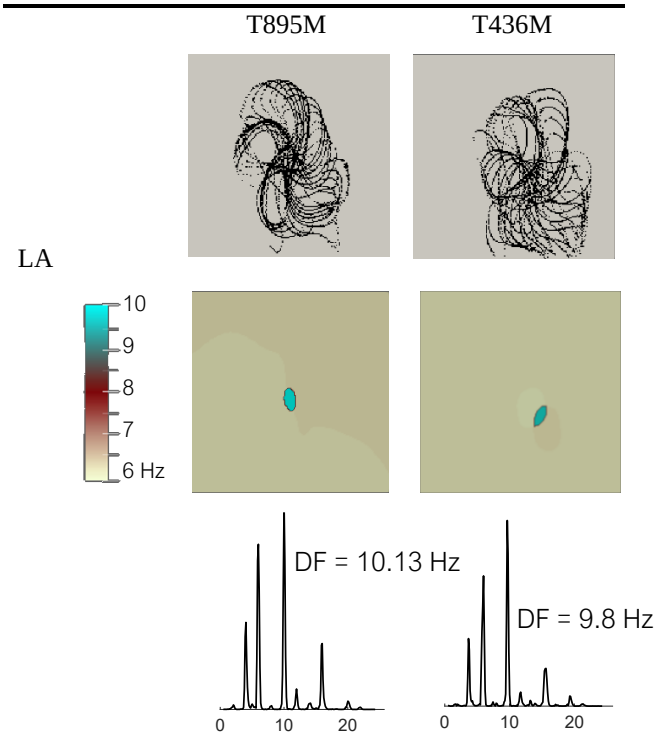

Table 3. *Upper panel: rotors' tip trajectory color-coded by ms of simulation. Middle panel: spatial distribution of high DF in the tissue. Lower panel: power spectrum of the two signals*

Temporal vulnerability of the tissue model to re entrant activities in presence of the two mutation studied revealed

that both of them were able to initiate a rotor, both in right and left atrium. However, not all the cases taken into consideration were able to maintain the spiral wave till the end of the simulation, which in this work has been set at 5 s. Re-entrant activities perpetuating till the end of the simulation have been observed in presence of both mutation in LA. Spectral analysis has been performed and dominant frequency values were equal to 9.8 Hz in T895M case and 10.13 Hz in T436M case. Information about the DF spatial distribution indicates that higher DF areas coincide with the central areas of rotors' meandering as shown in ***Table 3.***'s middle panel. Phase analysis provided information about temporal distribution of singularity points, allowing the tracking of the rotors' tip trajectory during the 5s-simulation. Rotor's meandering area is less extended in presence of T895M rather than in presence of T436M and, as it can be appreciated in the upper panel of ***Table 3.***, the pattern seems quite regular in T895M condition, if compared with T436M case.

4. Discussion and Conclusions

The simulation study presented in this paper proposed to characterize the effects of two gain-of-functions genetic mutations, T895M and T436M, found in patients affected by AF. With this aim, a parameter estimation procedure has been performed to incorporate mutant experimental datasets into a well-established human atrial myocyte model. Using an adaptive heuristic search method, the genetic algorithm, mutation data were successfully fitted and pathological channel dynamics were reproduced. Single cell and tissue patch simulations have been thus carried out in order to further understand the mechanisms behind these pathological conditions. 0D simulations revealed both genetic mutations led to an APD_{90} reduction, an increased I_{Kr} peak and to a shift to low APD values in the APDr. These effects were more pronounced in presence of the mutation T895M, rather than in presence of the mutation T436M; in particular, the former defects was also responsible for an APDr flattening, with a reduction in the maximum slope value, while the latter did not affect it at all. Both APD_{90} shortening and resistance to high frequency pacing excitations have been demonstrated to be related to the generation of a substrate more prone to re entrant activity initiation and progression [8]. Simulations on a two-dimensional tissue model confirmed this assumption. In presence of both mutations, spiral waves had been induced, but only in left atrium they could be maintained for the whole simulation time. The study of singularity points allowed to keep track of rotor's tip trajectory which were more regular in shape and less extended in area in T895M case, with respect to T436M case. Dominant frequencies are spatially organized in the areas of the meandering rotors' centres and DF values lied in the range of values reported in literature for subject suffering from paroxysmal and permanent AF [9]. Further investigation of the system affected by these pathological conditions will be necessary in order to better assess and characterize the effects on whole – atrial and torso geometries. The importance of an accurate modelling and study of these rare mutations are highlighted by the fact that even if they affect the same channel portion, different mutations can lead to different dynamical impairments, which will require different therapeutic strategies, including a patient-specific design of targeted drug therapies.

Acknowledgements

I am grateful to the teams at GaTech, who helped me in the realization of this work. This project has been funded by the European Union's Horizon 2020 research and innovation programme under the Marie Skłodowska-Curie gran agreement No.766082 and by Generalitat Valenciana, Prometeo programme 2020/043.

References

[1] A. A. Y. Ragab, G. D. S. Sitorus, B. B. J. J. M. Brundel, and N. M. S. de Groot, "The Genetic Puzzle of Familial Atrial Fibrillation," *Front. Cardiovasc. Med.*, vol. 7, no. February, pp. 1–8, 2020, doi: 10.3389/fcvm.2020.00014.

[2] I. E. Christophersen and P. T. Ellinor, "Genetics of atrial fibrillation: From families to genomes," *J. Hum. Genet.*, vol. 61, no. 1, pp. 61–70, 2016, doi: 10.1038/jhg.2015.44.

[3] D. Fatkin, R. Otway, and J. I. Vandenberg, "Genes and atrial fibrillation: A new look at an old problem," *Circulation*, vol. 116, no. 7, pp. 782–792, 2007, doi: 10.1161/CIRCULATIONAHA.106.688889.

[4] K. Hayashi *et al.*, "Functional Characterization of Rare Variants Implicated in Susceptibility to Lone Atrial Fibrillation," *Circ. Arrhythmia Electrophysiol.*, vol. 8, no. 5, pp. 1095–1104, 2015, doi: 10.1161/CIRCEP.114.002519.

[5] M. Courtemanche, R. J. Ramirez, and S. Nattel, "Ionic mechanisms underlying human atrial action potential properties: insights from a mathematical model," *Am. J. Physiol. -Heart Circ. Physiol.*, vol. 275, pp. 301–321, 1998, doi: 10.1152/ajpheart.1998.275.1.H301.

[6] E. Grandi *et al.*, "Human atrial action potential and Ca 2+ model: Sinus rhythm and chronic atrial fibrillation," *Circ. Res.*, vol. 109, no. 9, pp. 1055–1066, 2011, doi: 10.1161/CIRCRESAHA.111.253955.

[7] E. A. Heidenreich, J. M. Ferrero, M. Doblaré, and J. F. Rodríguez, "Adaptive macro finite elements for the numerical solution of monodomain equations in cardiac electrophysiology," *Ann. Biomed. Eng.*, vol. 38, no. 7, pp. 2331–2345, 2010, doi: 10.1007/s10439-010-9997-2.

[8] U. Schotten, S. Verheule, P. Kirchhof, and A. Goette, "Pathophysiological mechanisms of atrial fibrillation: A translational appraisal," *Physiol. Rev.*, vol. 91, no. 1, pp. 265–325, 2011, doi: 10.1152/physrev.00031.2009.

[9] P. Sanders *et al.*, "Spectral analysis identifies sites of high-frequency activity maintaining atrial fibrillation in humans," *Circulation*, vol. 112, no. 6, pp. 789–797, 2005, doi: 10.1161/CIRCULATIONAHA.104.517011.